

and support of L. W. Doremus at the Engineering Sciences Laboratory, Picatinny Arsenal. The experimental assistance of S. DeFeo and P. Calella is gratefully acknowledged. Valuable conversations were held

with M. Cohen, H. Fritzsche, S. Ovshinsky, K. Boer, E. Fagen, R. Neale, and C. Holz. Energy Conversion Devices graciously supplied technical data on their devices and on their bulk materials.

PHYSICAL REVIEW

VOLUME 178, NUMBER 3

15 FEBRUARY 1969

Electronic Structure and Optical Properties of SnS_2 and SnSe_2 †

M. Y. AU-YANG*

Department of Physics, University of California, Berkeley, California 94720

AND

MARVIN L. COHEN‡

Department of Physics and Inorganic Materials Division, Lawrence Radiation Laboratory, University of California, Berkeley, California 94720

(Received 3 September 1968)

The electronic band structures of SnS_2 and SnSe_2 are calculated by using the empirical pseudopotential method. The potentials were obtained by scaling those used in other energy-band calculations. The symmetry properties of the crystals are treated in detail, and the optical constants are calculated. Comparison with experiment is also made.

I. INTRODUCTION

THE concept of associating a pseudopotential with each ion core independent of its chemical state has been successfully exploited recently to yield electronic states of semiconductors both in elemental¹ and in compound forms.^{2,3} In the first case, the elemental pseudopotential is extracted from semiconductors containing that element, e.g., Se from ZnSe .¹ In the second case, the pseudopotential form factors in a compound are derived from the known pseudopotentials of the constituent elements, e.g., Mg and Si, to give Mg_2Si .² In these calculations, the empirical pseudopotential method⁴ (EPM) is used. The combination of assigning a fixed pseudopotential to each ion and the use of the EPM, then, essentially involves the variation of pseudopotential form factors to fit optical data and the existing information on the pseudopotentials.

The success we have had in the Mg_2X calculations³ and the availability of good optical data have stimulated us to attempt calculations of the electronic structure of SnS_2 and SnSe_2 . The similarity of these two classes of compounds, Mg_2X and SnX_2 , lies in the shape of the unit molecule: A dumbbell formed from the two identical atoms weighted at the center by the third, different

atom. This structure preserves the inversion symmetry of the lattice. This yields a Hamiltonian with real matrix elements which is easier to diagonalize than one with complex matrix elements. In addition to calculating the electronic structure of SnS_2 and SnSe_2 , we have also determined the optical constants for these materials.

The properties of SnS_2 and SnSe_2 have only been sporadically investigated experimentally and, to our knowledge, no band-structure calculations exist. The direct and indirect energy gaps of SnS_2 have been measured optically,^{5,6} and those of SnSe_2 have been measured both optically⁵ and electrically.^{7,8} The combined data seem to have fixed the energy gaps to within a small range of values. Reflectivity data in the range of 1 to 12 eV have also been obtained for SnS_2 , for light with polarization perpendicular to the *c* axis of the crystal.⁶

The pseudopotentials of the constituent ions in the calculation, i.e., those of Sn, Se, and S, are not available to a high degree of accuracy as are those of the group-IV elements, Si and Ge. The pseudopotential for Sn, for example, differs greatly between grey tin⁴ and white tin,⁹ especially for large $|G|$ values. We have based our calculations on the Sn, Se pseudopotentials of Animalu and Heine,⁹ and the S pseudopotential as extracted from ZnS .⁴

† Supported in part by the National Science Foundation.

* Present address: Research Laboratories, Eastman Kodak Co., Rochester, N. Y. 14615.

‡ Alfred P. Sloan Foundation Fellow.

¹ R. Sandroch, *Phys. Rev.* **169**, 642 (1968).

² M. Y. Au-Yang and M. L. Cohen (to be published).

³ M. Y. Au-Yang and M. L. Cohen, *Phys. Rev.* **178**, 1358 (1969).

⁴ M. L. Cohen and T. K. Bergstresser, *Phys. Rev.* **141**, 789 (1966).

⁵ G. Domingo, R. S. Itoga, and C. R. Kannewurf, *Phys. Rev.* **143**, 536 (1966).

⁶ D. I. Greenaway and R. Nitché, *J. Phys. Chem. Solids* **26**, 1445 (1965).

⁷ S. Asanabe, *J. Phys. Soc. Japan* **16**, 1789 (1961).

⁸ G. Busch, C. Frohlich, and F. Hulliger, *Helv. Phys. Acta* **34**, 359 (1961).

⁹ A. O. E. Animalu and V. Heine, *Phil. Mag.* **12**, 1249 (1965).

This paper is divided into three sections. In Sec. II the group theory of the CdI_2 structure is treated in detail, and the Hamiltonian is derived. The resulting Schrödinger equation is solved, and the optical constants are calculated. In Sec. III we present the results and the comparison with experiment.

II. CALCULATIONS

The tin chalcogenides, SnS_2 and SnSe_2 , crystallize in the CdI_2 structure. The lattice is simple hexagonal with one molecule per primitive cell. If one chooses the position of a Cd atom at the origin of the cell, then the positions of the I atoms can be chosen to be at the symmetric points $\pm \mathbf{u}$, where $\mathbf{u} = (\frac{2}{3}, \frac{1}{3}, \frac{1}{2})$. (In writing the vector we have assumed the usual hexagonal coordinate system of two $|\mathbf{a}|$ vectors on the x,y plane placed 120° apart and a \mathbf{c} vector in the z direction, where a and c are the usual lattice constants.) The symmetry of the lattice is D_{6h} ; however, because of the basis, only 4 of the 24 symmetry operations in D_{6h} leave the structure invariant. These are the identity, a two-fold rotation about a corner of the hexagon in the x,y plane, inversion, and finally a reflection in the plane perpendicular to the two-fold axis. [See Fig. 1(a).]

The first Brillouin zone of the hexagonal unit cell is again a hexagonal prism; however, as a consequence of the basis atoms in the CdI_2 structure, the six sides of

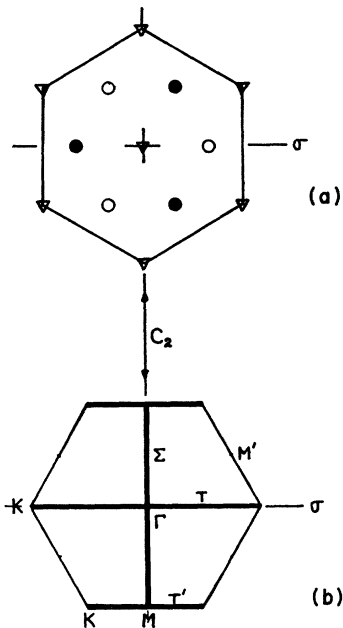


FIG. 1. (a) Projection on the x,y plane of the CdI_2 structure in real space. The triangles denote the positions of the Cd atoms, and the circles denote those of the I atoms. The triangles are on the x,y plane; the open and the closed circles are on the planes $z = \pm \frac{1}{2}c$, respectively, where c is the usual lattice constant. (b) Section of the first Brillouin zone of the simple hexagonal lattice on the x,y plane. The symmetry lines for the CdI_2 structure are labelled and they are drawn in heavy lines. The twofold axis and the reflection planes are indicated by C_2 and σ in both figures.

the hexagon are no longer equivalent. In fact, the direction of the two-fold axis in real space is the particular direction in the reciprocal space. It passes through the center of the zone and the midpoint of one side of the hexagon on the x,y plane (and also that of the opposite side). [See Fig. 1(b).] These two points, called M points in the usual notation, are the only M points which are invariant under C_2 in the CdI_2 structure. The other M points are only invariant under inversion. We, therefore, call the M points with lower symmetry M' points.

It is easily seen from Fig. 1(b) that except for the M' points, all other points of symmetry are on three symmetry lines and three symmetry planes. The symmetry lines are the C_2 axis (Σ line) and the two lines parallel to it and displaced by $\pm \pi/c$ in the c direction (R lines). The symmetry planes are perpendicular to the C_2 axis; they include two planes which contain the two pre-

TABLE I. Characters of the small representations of $\Gamma, A, M, L, P, \Sigma$, and R , where P is a general point on a symmetry plane. z and x,y rows show the characters for the photons with polarizations perpendicular and parallel to the c axis.

Γ, A, M, L	E	c_2	I	σ
Γ_1	1	1	1	1
Γ_2	1	-1	1	-1
Γ_1'	1	-1	-1	1
Γ_2'	1	1	-1	-1
x,y	2	0	-2	0
z	1	-1	-1	1
P				
P_1	1			1
P_2	1			-1
x,y	2			0
z	1			1
Σ, R				
Σ_1	1	1		
Σ_2	1	-1		
x,y	2	0		
z	1	-1		

viously mentioned special M points, and the third plane passes through the origin, the Γ point. The intersection of these planes and the x,y plane are the T and T' lines. The symmetry at Σ and R is the group C_2 , and that at T, T' is the group C_s . The intersection of these lines and planes are the Γ, A, L , and M points. These points, therefore, have the highest symmetry in the structure, the group $C_2 \times C_s$.

From the above discussion we see that the group theoretical treatment of the CdI_2 structure is quite simple. There are only three important types of symmetry points, and the compatibility relations between them are trivial since we only have four symmetry operations. In Table I, the characters are given for the symmetry operations of the three groups and the irreducible representations are defined. The symmetry points M' are not considered because they have a low symmetry and are not joined by other symmetry points.

To calculate the optical properties of the CdI_2 structure, we need to have the selection rules for optical transitions with the electric field vector both in the directions parallel and perpendicular to the \mathbf{c} axis. In Table I, the characters for photons with both types of polarizations are given. From these characters, it is easy to compute the selection rules given in Table II.

This completes our discussion of the group theoretical aspects of the problem; next, we derive the Hamiltonian and solve the Schrödinger equation.

We use an energy-independent pseudopotential and neglect the spin-orbit interaction; the pseudo-Hamiltonian then becomes

$$\mathcal{H} = -(\hbar^2/2m)\nabla^2 + V(\mathbf{r}). \quad (1)$$

Expanding the potential in the reciprocal lattice, we have

$$V(\mathbf{r}) = \sum_{\mathbf{G}} V(\mathbf{G})e^{i\mathbf{G}\cdot\mathbf{r}}, \quad (2)$$

and so

$$V(\mathbf{G}) = \frac{1}{\Omega_{\text{cell}}} \int_{\text{cell}} V(\mathbf{r})e^{-i\mathbf{G}\cdot\mathbf{r}} \\ = \frac{1}{\Omega_{\text{cell}}} [\Omega_{\text{Cd}}V^{\text{Cd}}(\mathbf{G}) + 2\Omega_{\text{I}}V^{\text{I}}(\mathbf{G}) \cos(\mathbf{G}\cdot\mathbf{u})], \quad (3)$$

where the Ω 's with subscripts denote the volumes per molecule or atom in CdI_2 , Cd, and I and the V 's with superscripts denote the pseudopotentials of the constituent ions Cd and I. [For the actual case of CdI_2 , in which I_2 is a gas, we can define $V^{\text{I}}(\mathbf{G})$ without the $1/\Omega_{\text{I}}$ factor, thus getting rid of the ambiguous quantity Ω_{I} .] The factor $\cos(\mathbf{G}\cdot\mathbf{u})$ includes all the effects of the basis atoms and accounts for the destruction of most of the symmetries of the lattice.

The Schrödinger equation with this Hamiltonian Eq. (1) is solved by expanding the periodic part of the Bloch state in plane waves. For SnS_2 and SnSe_2 , the calculations present a convergence problem if we use the full pseudopotential curves of the constituent ions. The reason is that the hexagonal lattice contains many plane waves with small values of $|\mathbf{G}|$, and therefore the pseudopotential curves must be cut off for some maximum $|\mathbf{G}|$ value, determined by the accuracy of the computer available for the diagonalization of the Hamiltonian. The value we chose was $G_{\text{max}} = (59/4) \times (2\pi^2/a^2)$. (This is for $(c/a)^2 = 8/3$, which is approximately valid in both SnS_2 and SnSe_2 .) This value of G_{max} gives 16 nonvanishing pseudopotential form factors for Sn.

The Hamiltonian is diagonalized on a mesh of \mathbf{k} points $\frac{1}{4}$ the size of the Brillouin zone. The band structure thus obtained is used to calculate the optical constants of these materials.¹⁰ The first optical constant

¹⁰ T. K. Bergstresser and M. L. Cohen, Phys. Rev. **164**, 1069 (1967).

TABLE II. Selection rules for direct optical transitions. For points of the same symmetry, only one point is shown (i.e., Γ represents Γ , Δ , M , and L).

<i>Perpendicular polarization</i>	
$\Gamma_1, \Gamma_2 \leftrightarrow \Gamma_1', \Gamma_2'$	
$P_1, P_2 \leftrightarrow P_1, P_2$	
$\Sigma_1, \Sigma_2 \leftrightarrow \Sigma_1, \Sigma_2$	
<i>Parallel polarization</i>	
$\Gamma_i \leftrightarrow \Gamma_i'$	
$P_i \leftrightarrow P_i$	
$\Sigma_i \leftrightarrow \Sigma_j$	
where $i \neq j$ and $i = 1, 2$	

to be calculated is the imaginary part of the dielectric functions $\epsilon_2(\omega)$. The computation uses the equation

$$\epsilon_2(\omega) = \frac{e^2 \hbar^2}{\theta \pi m^2 \omega^2} \sum_{c,v,i} \int \delta(E_c(\mathbf{k}) - E_v(\mathbf{k}) - \hbar\omega) \\ \times \left| \left\langle u_{\mathbf{k},v} \left| \frac{d}{dx_i} \right| u_{\mathbf{k},c} \right\rangle \right|^2 d^3k, \quad (4)$$

where c, v denotes the conduction and valence bands, and $u_{\mathbf{k},n}$ is the periodic part of the n th-band wave function. $\theta = 2$, $i = 1, 2$ for light with polarization perpendicular to the \mathbf{c} axis, and $\theta = 1$, $i = 3$ for light with parallel polarization. We shall approximate the wave functions $u_{\mathbf{k},n}$ by the eigenstates of the pseudo-Hamiltonian, Eq. (1).

Before we discuss the results of the calculation, we would like to emphasize that, because of several difficulties, the calculations should be regarded as being preliminary. In terms of accuracy they cannot be compared with the calculations performed on the Mg_2X compounds, for example. The difficulties with SnS_2 and SnSe_2 calculations are as follows:

(a) The low symmetry of the CdI_2 structure necessitates the computation of the band structure in $\frac{1}{4}$ the Brillouin zone which is six times as large as the amount of \mathbf{k} space required for the wurtzite compounds.¹⁰ The unusually large matrices to be diagonalized in the hexagonal lattice makes an accurate calculation impractical at this stage.

(b) Although reflectivity data on SnS_2 are available, an $\epsilon_2(\omega)$ curve is not yet available. The lack of this curve makes it quite difficult to correlate the results of theory with experiment. In addition, no spectrum for SnSe_2 is available.

(c) There are eight valence bands, six of which are important for optical transitions under 12 eV. In addition, we have to take into account ten conduction bands for our final states in the optical transitions. The large number of bands contributing to $\epsilon_2(\omega)$ makes the identification of the theoretical $\epsilon_2(\omega)$ in terms of critical points quite difficult.

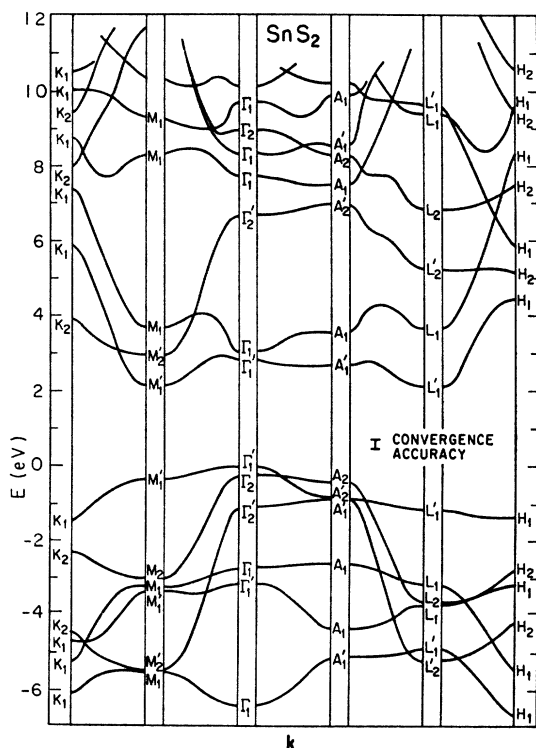


FIG. 2. Calculated band structure of SnS_2 . The first two bands are not shown; they are lower than the third band by at least 4.5 eV.

In view of these difficulties, little attempt has been made to adjust the potentials. The agreement between theory and experiment is therefore not expected to be better than 0.5 to 1.0 eV.

TABLE III. Pseudopotential form factors in Ry used in the calculations of the SnS_2 and SnSe_2 band structures. The Sn potentials for both compounds are identical. The differences in the table arise because of lattice-constant differences.

G	SnS_2 :Sn	S	SnSe_2 :Sn	Se
(001)	-0.312	...	-0.36	...
(100)	-0.09	-0.31	-0.06	-0.24
(002)	-0.06	-0.27	-0.036	-0.205
(101)	-0.036	-0.21	-0.024	-0.17
(102)	0.06	-0.08	0.072	-0.012
(003)	0.074	-0.042	0.074	0.03
(210)	0.075	-0.012	0.073	0.08
(211)	0.074	0.004	0.071	0.10
(103)	0.073	0.032	0.069	0.12
(200)	0.068	0.082	0.057	0.14
(212)	0.066	0.088	0.054	0.14
(201)	0.065	0.096	0.05	0.13
(004)	0.06	0.102	0.048	0.11
(202)	0.048	0.074	0.035	0.08
(104)	0.036	0.054	0.029	0.05
(213)	0.036	0.05	0.029	0.05

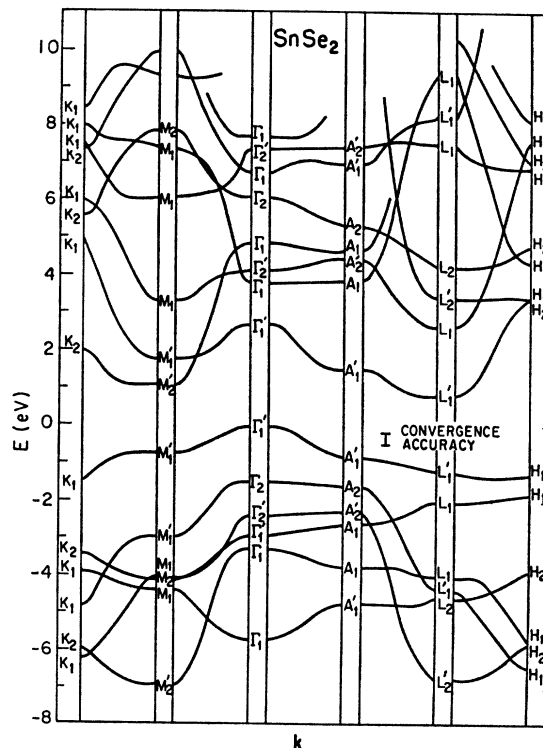


FIG. 3. Calculated band structure of SnSe_2 . As in Fig. 2, the first two bands are not shown.

III. RESULTS AND DISCUSSION

The band structures of SnS_2 and SnSe_2 are shown in Figs. 2 and 3 along certain symmetry directions of the hexagonal lattice. The pseudopotential form factors used in the calculations are shown in Table III. As previously mentioned, some of the special labels (for example, K) in the hexagonal lattice have no particular importance here. They are shown mainly to illustrate how the bands appear along selected general directions.

For both SnS_2 and SnSe_2 , the direct and indirect energy gaps are fitted to experiment. In addition, for SnS_2 , the optical spectrum was used to fix some of the high-energy splittings. We again remark that in both cases the potentials chosen were constrained to match those derived from analysis of other crystals.

TABLE IV. Comparison between theory and experiment for the direct and indirect threshold energy gaps (given in eV).

	Direct		Indirect	
	Calculated	Measured	Calculated	Measured
SnS_2 : 2.48		2.88 ^a	SnS_2 : 2.11	2.07 ^a
$(M_1' \rightarrow M_1')$			$(\Gamma_1' \rightarrow L_1')$	2.21 ^b
SnSe_2 : 1.78		1.62 ^a	SnSe_2 : 0.81	0.97 ^a
$(M_1' \rightarrow M_2')$			$(\Gamma_1' \rightarrow L_1')$	1.0 ^c
				1.0 ^d

^a Reference 5.
^b Reference 6.
^c Reference 7.
^d Reference 8.

TABLE V. Some dominant optical transitions for perpendicular polarization in SnS_2 and comparison with experiment. The subscripts in the optical transition labels indicate the band indices for the transition. The peak labels for the measured reflectivity curves are from Ref. 6.

Energy value of structure		Identification of main transition in calculated $\epsilon_2(\omega)$	Type of cp
In the measured reflectivity (eV)	In the calculated $\epsilon_2(\omega)$ (eV)		
4.0 (A)	4.03	$(M_1' \rightarrow M_1)_{8,11}$	M_0
4.8 (B)	5.35	$(M_1 \rightarrow M_1')_{6,9}$	M_1
5.7 (C)	5.83	$(L_1 \rightarrow L_1')_{5,9}$	M_1
7.0 (D)	7.72	$(\Gamma_1' \rightarrow \Gamma_1)_{8,12}$	M_0
7.8 (E)	8.67	$(M_1' \rightarrow M_1)_{8,12}$	M_1

The direct energy gaps for both SnS_2 and SnSe_2 are the results of transitions near the M point between the eighth and the ninth bands; the calculated values are 2.48 eV (SnS_2) and 1.78 eV (SnSe_2). The calculated transition at the M point itself is forbidden by parity. Experimentally, the threshold for direct transition for both compounds is forbidden as is suggested by the absorption data of Domingo *et al.*⁵ They obtained direct energy gaps (forbidden in first order) of 2.88 eV and 1.62 eV for SnS_2 and SnSe_2 , respectively.

The calculated fundamental energy gaps of both compounds are indirect. The maximum of the valence band is at Γ , and the minimum of the conduction band is at L . This fact seems to be well supported by experiment.^{5,6} The calculated values are 2.11 and 0.81 eV for SnS_2 and SnSe_2 , which compare fairly well with the average experimental values of 2.14 and 0.99 eV⁵⁻⁸ (see Table IV).

The imaginary part of the dielectric function $\epsilon_2(\omega)$ calculated from the band structure of SnS_2 is shown in Fig. 4 for light polarization both parallel and perpendicular to the c axis. In Table V some prominent peaks in the reflectivity data of Greenaway and Nitsche⁶ are compared with the results of the calculation. Because of the difficulties encountered in calculations, as mentioned in Sec. II, not much effort has been made to fit the

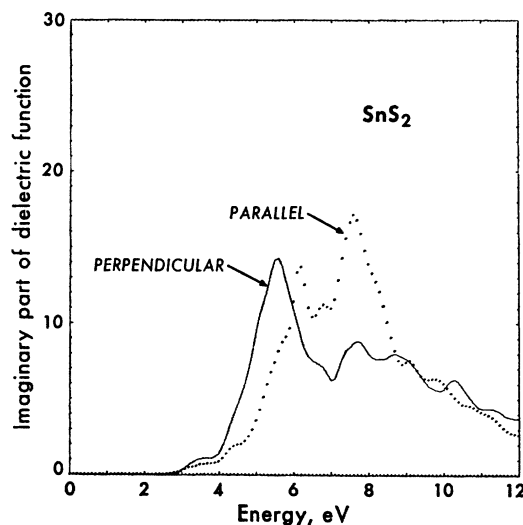


FIG. 4. Calculated imaginary part of the dielectric function for light polarizations perpendicular and parallel to the c axis, for SnS_2 .

theory to the experiment to better than 1.0 eV, and only the most important critical points (cp) are identified for each peak. We remark, also, that because of the low symmetry of the structure, a great deal of contribution to the $\epsilon_2(\omega)$ comes from "volume effects," i.e., contributions which are not related to a cp. We note that all transitions which are allowed in parallel polarization are also allowed in perpendicular polarization. If in the experiments⁶ on SnS_2 the light were not completely polarized perpendicular to the c axis, then the peak labelled C in Ref. 6 would be larger than expected for purely perpendicularly polarized light. This would make the comparison between theory and experiment much better.

ACKNOWLEDGMENTS

We would like to thank W. Saslow and Dr. S. Bowen for helpful discussions.